ELSEVIER

Journal of Organometallic Chemistry 563 (1998) 1–6

Journal of Organometallic Chemistry

Oxidation of $Ru(dppe)(CO)_3$ with *o*- and *p*-quinones. Crystal structure of $\overline{Ru[C(O)OC_6H_2(C_4H_9)_2O]}(dppe)(CO)_2$

Amy L. Jorgenson, Robert A. Nadeau, Victor G. Young Jr., Wayne L. Gladfelter *

Department of Chemistry, University of Minnesota, 207 Pleasant Street SE, Minneapolis, MN 55455, USA

Received 2 February 1997; received in revised form 9 February 1998

Abstract

The oxidation of $Ru(dppe)(CO)_3$ with various *o*- and *p*-quinones is described. Reaction with 3,5-di-*t*-butyl-*o*-benzoquinone yielded a metallacyclic complex which crystallizes in the monoclinic space group $P2_1/c$ with $a = 21.8388$ (1), $b = 12.0734$ (1), $c = 17.6173$ (3) Å, $\beta = 105.549$ (1), and $Z = 4$. The complex exhibited slightly distorted octahedral geometry and contained a puckered metallacyclic ring resulting from the formal addition of the *o*-quinone moiety across the Ru–C bond of a metal carbonyl. Reaction of this quinone adduct with an alkylamine produced a known bis(carbamoyl) complex, $Ru(dppe)(CO)_2[C(O)NHR]_2$. The reaction of $Ru(dppe)(CO)_3$ with *p*-quinones generated unidentified oxidation products which exhibited a similar reactivity with amines to form bis(carbamoyl) complexes.

Keywords: Crystal structure; Oxidation; Quinones

1. Introduction

The oxidative carbonylation of alkylamines has been studied as a phosgene-free route to dialkyl ureas [1–11]. We discovered that the reaction shown in Eq. (1) is

$$2RNH_2 + 3CO + ArNO_2 \rightarrow ArNH_2 + 2CO_2 + RNHC(O)NHR \quad (1)$$

catalyzed by $Ru(dppe)(CO)_3$ (**1**), where the nitroaromatic compound serves as the oxidant. Though an efficient oxidant in this system, the use of nitroarenes is not desirable due to the cost, toxicity and the by-product, aniline, generated during the reaction.

Quinones exhibit redox activity at accessible potentials and form complexes with various transition metals, [12–17] including ruthenium [18–26]. They have also been successfully used in so-called 'triple catalysis' schemes in which the quinone is used to oxidize a transition metal catalyst and is itself regenerated by molecular oxygen [27,28]. For these reasons, quinones may be a good replacement for nitrobenzene as an oxidant for the catalytic system shown in Eq. (1), and to explore this possibility we have studied the reaction of *o*- and *p*-quinones with **1**.

2. Experimental section

2.1. General

Standard Schlenk techniques were used in preparing all organometallic compounds. A nitrogen-filled MBraun dry box equipped with an inert gas purifier was used for manipulations carried out in the glove box. $Ru_3(CO)_{12}$ and 1,2-bis(diphenylphosphino)ethane were purchased from Strem Chemicals with the latter being purified by recrystallization from toluene/hexane. $Ru(dppe)(CO)_3$ (**1**) was prepared using literature methods [29,30]. The *p*-benzoquinone was sublimed under vacuum and stored in a refrigerator in the glove box. Anthraquinone and 1,8-dichloroanthraquinone were re-

* Corresponding author. Tel.: +1 612 6244391; fax: +1 612 6267541; e-mail: gladfelt@chem.umn.edu

0022-328X/98/$19.00
PII S0022-328X(98)00537-3

crystallized from hot benzene, and all other quinones were recrystallized from ethanol and dried under vacuum. Toluene, tetrahydrofuran (THF), and hexane were distilled prior to use from sodium benzophenone ketyl; methylene chloride and deuterated methylene chloride were distilled from calcium hydride.

All infrared spectral measurements were carried out on a Mattson Polaris FTIR spectrometer. The ^{1}H-, ^{13}C-, and ^{31}P-NMR studies were performed using a Varian Unity 300 MHz spectrometer. All ^{31}P-NMR spectra were externally referenced to 85% H_3PO_4. Elemental analyses were measured by M-H-W Laboratories.

2.2. Reaction of **1** with *p*-quinones

In a typical reaction of **1** with *p*-quinones, a Schlenk tube equipped with a stir bar was charged with **1** (100 mg, 171 mmol) and the *p*-quinone in a 2:1 ratio of quinone:**1**. THF (10 ml) was then added to the reaction flask, and the reaction progress was monitored by IR spectroscopy. The following *p*-quinones were tested in this manner: *p*-benzoquinone, 2,5-dimethylbenzoquinone, 2,6-dimethylbenzoquinone, duroquinone, anthraquinone, 1,8-dichloroanthraquinone, 2,3-dichloro-1,4-napthoquinone, 2,5-dichlorobenzoquinone and *p*-chloranil.

2.3. Reactivity of oxidation products. A. In situ reaction of **1** with *p*-chloranil and isobutylamine

A 50 ml round bottom flask was loaded with **1** (107 mg, 0.183 mmol) and *p*-chloranil (55 mg, 0.224 mmol). The flask was sealed with a septum, removed from the box and 10 ml of THF, and 0.5 ml of isobutylamine (5 mmol) were injected into the flask. After 5 min, **1** had been completely converted to a bis(carbamoyl) complex, $Ru(dppe)(CO)(RNH_2)[C(O)NHR]_2$ (**4**), as observed by the appearance of the ν_{CO} at 1915 cm^{-1} in the IR spectrum.

2.4. B. Isolation of oxidation product and subsequent reaction with isopropylamine and isobutylamine

A 50 ml round bottom Schlenk flask was charged with **1** (150 mg, 0.257 mmol) and *p*-benzoquinone (38 mg, 0.352 mmol). To this was added 10 ml of THF and the reaction was allowed to stir for 1.5 h at room temperature. The oxidation product was isolated by reducing the volume of the reaction solution by one-half and adding 5 ml of hexane. The resulting yellow–gold solid was collected on a Schlenk frit and dried in vacuo (154 mg).

A portion of the product from this reaction (23 mg) was dissolved in 6 ml THF in a Schlenk tube. Isopropylamine (0.5 ml, 6 mmol) was added to the solution and the reaction was monitored by IR and ^{31}P-NMR spectroscopy. After 1 h, the complex had been quantitatively converted to a bis(carbamoyl) complex, $Ru(dppe)(CO)_2[C(O)NHR]_2$ (**3**), [31] along with production of hydroquinone as observed by ^{1}H-NMR spectroscopy.

The reactivity of this oxidation product was also studied with isobutylamine. A sample of the *p*-benzoquinone oxidation product (63 mg) was placed in a 50 ml round bottom Schlenk flask and dissolved in 9 ml of THF. To this solution isobutylamine (0.5 ml, 5 mmol) was added. The reaction was monitored by IR spectroscopy and after 10 min the *p*-benzoquinone complex had been completely converted to **4**, [32] along with evolution of hydroquinone. The products were verified by ^{31}P- and ^{1}H-NMR spectroscopy.

2.5. Synthesis of **2**

In the dry box, **1** (0.15 g, 0.26 mmol) and 3,5-di-*t*-butyl-*o*-quinone (0.056 g, 0.27 mmol) were placed into a 50 ml round bottom Schlenk flask with a stir bar. This flask was then sealed, removed from the dry box and 10 ml of THF was injected into the flask. This was allowed to stir for ca. 35 min before IR spectroscopy verified the reaction had gone to completion. Hexane (10 ml) was added, and an off-white precipitate formed. The precipitate was collected on a Schlenk frit assembly, washed with hexane (2×5 ml) and dried under vacuum to yield 0.054 g of **2** (26.2% yield). IR ν_{CO} (cm^{-1}, THF): 2051 (s), 1983 (s), 1652 (m), 1560 (w). ^{1}H-NMR δ (ppm, CD_2Cl_2): 8.05 (m, ArH), 7.7 (m, ArH), 7.55 (m, ArH), 7.4 (m, ArH), 7.2 (m, ArH), 6.6 (d, $J_{HH} = 2.38$ Hz, ArH), 5.87 (d, $J_{HH} = 2.38$ Hz, ArH), 3.0 (m, CH_2), 1.40 (s, CH_3), 1.18 (s, CH_3). ^{31}P{^{1}H}-NMR δ (ppm, CD_2Cl_2): 44.8 (d, $J_{PP} = 14.0$ Hz), 37.7 (d, $J_{PP} = 14.1$ Hz). ^{13}C{^{1}H}-NMR (ppm, CD_2Cl_2): 201.5 (dd, $J_{CP1} = 105.1$ Hz, $J_{CP2} = 10.3$ Hz, CO), 197.1 (dd, $J_{CP} = 6.3$ Hz, $J_{CP} = 12.6$ Hz, CO), 194.2 (dd, $J_{CP1} = 8.2$ Hz, $J_{CP2} = 97.6$ Hz, CO), 32.0 (s, CH_3), 30.8 (s, CH_3), 26.1 (m, CH_2). Anal. calcd. for **2**: C, 64.25; H, 5.52. Found: C, 64.12; H, 5.54%.

2.6. Reaction of **2** with isobutylamine

Complex **2** (25 mg, 0.031 mmol) was placed in a 50 ml round bottom Schlenk flask and was dissolved completely in 6 ml of THF. Isobutylamine (0.5 ml, 5 mmol) was injected into the flask and the reaction was monitored by IR spectroscopy. After 5 min, **2** had completely reacted to form **4**, as observed in the IR spectrum. Spectroscopic data for **4**: IR ν_{CO} (cm^{-1}, THF): 1915 (s), 1608 (w), 1557 (m). ^{1}H-NMR δ (ppm, CD_2Cl_2): 7.82 (m, ArH), 7.61 (m, ArH), 7.38 (m, ArH), 5.70 (t, NH), 4.40 (br, NH_2), 3.20 (m, CH_2), 2.65 (m, CH_2), 1.78 (m, CH), 0.93 (d, CH_3), 0.80 (m, CH, CH_2),

0.22 (d, CH_3). $^{31}P\{^1H\}$-NMR δ (ppm, CD_2Cl_2): 39.1 (s). $^{13}C\{^1H\}$-NMR δ (ppm, CD_2Cl_2): 208.8 (dd, J_{CP}-cis = 9.2 Hz, $J_{CPtrans}$ = 90.3 Hz, CO), 205.0 (t, J_{CP} = 9.5 Hz, CO), 51.2 (s, CH_2), 47.3 (s, CH_2), 31.4 (s, CH), 29.1 (s, CH), 26.4 (m, CH_2), 20.3 (s, CH_3), 19.2 (s, CH_3).

2.7. X-ray crystallography of **2**

A crystal, grown from a CH_2Cl_2/hexane solution, was mounted on a glass fiber and cooled to −100°C for data collection. Table 1 contains a summary of the crystallographic data. The intensities were collected with a Siemens SMART Platform with Mo–K_α (λ = 0.71073 Å) radiation up to $2\theta = 50°$. A monoclinic cell was determined after a preliminary peak search. The data collection method involved examining a randomly oriented region of reciprocal space to a resolution of 0.84 Å. Data were collected over three regions with 0.30° steps in omega. A total of 21 504 reflections were collected with 7807 independent reflections used to calculate the structure.

Table 1
Summary of crystallographic data for 2

Crystal parameters	
Empirical formula	$RuC_{47}H_{53}P_2O_5Cl_2$
FW (g mol^{-1})	931.80
Crystal system	Monoclinic
Space group	$P2_1/c$
a (Å)	21.8388 (1)
b (Å)	12.0734 (1)
c (Å)	17.6173 (3)
α (°)	90
β (°)	105.549 (1)
γ (°)	90
V (Å^3)	4475.12 (9)
Z	4
ρ(calc) (g cm^{-3})	1.383
Crystal dimensions (mm)	0.35 × 0.12 × 0.05
Absorption coefficient (mm^{-1})	0.586
Measurement of intensity data	
Diffractometer	Siemens SMART Platform CCD
Radiation	Mo–K_α (λ = 0.71073 Å)
Monochromator	Graphite
Temperature (°C)	−100 (2)
Scan type	ω
No. reflections measured	21504
No. unique reflections	7807
Absorption correction	SADABS
Transmission factors (max/min%)	100/83.7
Solution and refinement	
Programs used	SHELXTL-V5.0
Method of solution	Direct methods
No. reflections used	7806
R indices ($I > 2\sigma(I)$)	0.0667
R indices (all data)	0.1263
Goodness-of-fit	1.047

Table 2
Selected bond distances (Å) and angles (°) for 2

A. Metal–Ligand distances			
Ru1–P1	2.410 (2)	Ru1–P2	2.410 (2)
Ru1–C1	1.934 (6)	Ru1–C2	1.873 (6)
Ru1–C3	2.088 (6)	Ru1–O5	2.082 (4)
B Intraligand distances			
P1–C61	1.825 (6)	P1–C71	1.831 (6)
P1–C81	1.833 (6)	P2–C41	1.815 (6)
P2–C51	1.821 (6)	P2–C82	1.828 (6)
C81–C82	1.532 (8)	C1–O1	1.136 (6)
C2–O2	1.144 (7)	C3–O3	1.211 (6)
C3–O4	1.407 (6)	O4–C11	1.390 (6)
C11–C16	1.416 (8)	C16–O5	1.342 (6)
C. Ligand–metal–ligand angles			
P1–Ru1–P2	82.45 (6)	P1–Ru1–C1	177.5 (2)
P1–Ru1–C2	94.0 (2)	P1–Ru1–C3	88.7 (2)
P1–Ru1–O5	85.55 (10)	P2–Ru1–C1	95.8 (2)
P2–Ru1–C2	93.7 (2)	P2–Ru1–C3	169.6 (2)
P2–Ru1–O5	86.92 (12)	C1–Ru1–C2	88.4 (2)
C1–Ru1–C3	91.8 (2)	C1–Ru1–O5	92.0 (2)
C2–Ru1–C3	93.7 (2)	C2–Ru1–O5	179.2 (2)
C3–Ru1–O5	85.7 (2)		
D. Intraligand angles			
Ru1–P1–C81	104.8 (2)	Ru1–P2–C82	107.0 (2)
Ru1–C1–O1	177.1 (5)	Ru1–C2–O2	177.5 (5)
Ru1–C3–O3	128.0 (4)	Ru1–C3–O4	118.1 (4)
C3–O4–C11	125.1 (4)	O4–C11–C16	120.8 (5)
C16–O5–Ru1	114.9 (3)	P1–C81–C82	109.7 (4)
P2–C82–C81	110.0 (4)		

All calculations were performed using the SHELXTL-Plus V5.0 [33] crystallographic software package. The structure was solved by direct methods and refined by full-matrix least-squares on F^2. The space group $P2_1/c$ was chosen based on systematic absences and was successfully used to solve the structure. All non-hydrogen atoms were refined anisotropically. The hydrogen atoms were placed in ideal positions and refined as riding atoms with relative isotropic displacement parameters.

One molecule each of dichloromethane and hexane were located within the structure. The molecule of hexane appears to shift along the length of the cavity in which it resides and was modeled as a half-occupied n-hexane. The disorder present in the molecule of hexane led to residuals higher than expected for this structure. Selected bond lengths and angles of **2** are listed in Table 2 and the molecular structure of **2** is shown in Fig. 1.

3. Results and discussion

The reaction between **1** and p-benzoquinone proceeds cleanly as observed in the IR spectrum which shows two peaks in the carbonyl region at 2050 and 1976 cm^{-1} typical of neutral cis-carbonyl Ru^{2+} com-

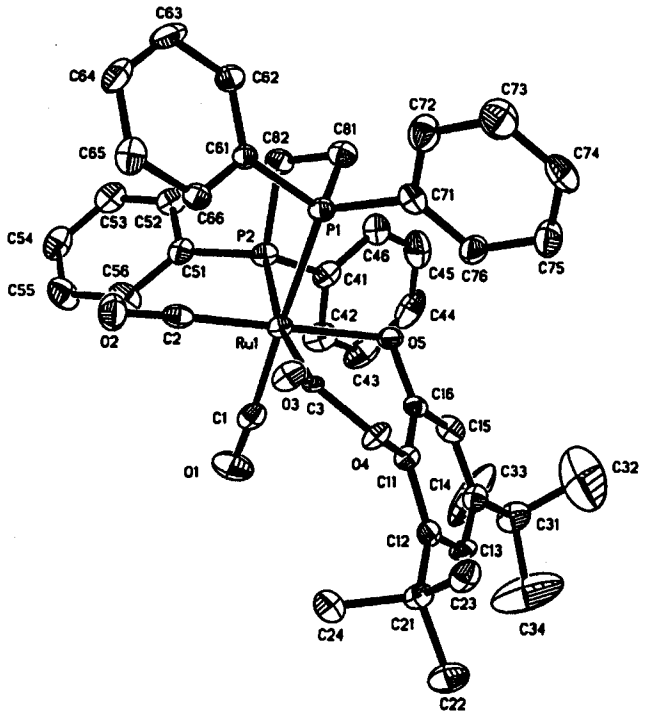

Fig. 1. Molecular structure and atom labeling of **2**. Atoms are depicted as 50% probability ellipsoids with hydrogen atoms omitted.

plexes. The stoichiometry of this reaction was found to be 1:1, suggesting a simple adduct formation between **1** and *p*-benzoquinone. However, inspection of the ^{31}P-NMR spectrum shows a mixture of products which have similar chemical shifts and coupling constants.

When this mixture was allowed to react with isopropylamine, two large peaks were observed in the ν_{CO} region of the IR spectrum at 2024 and 1969 cm^{-1}. The ^{1}H-NMR spectrum of the reaction products identified the organic product to be hydroquinone. A ^{31}P-NMR spectrum of the reaction products showed two doublets at 56.5 ($J_{PP} = 12.9$ Hz) and 53.4 ppm ($J_{PP} = 12.7$ Hz), establishing the major organometallic product to be a bis(carbamoyl) complex, Ru(dppe)(CO)$_2$[C(O)NHR]$_2$ (**3**), as shown in Scheme 1. This bis(carbamoyl) complex had been previously synthesized through independent routes [31,32] and is proposed as an intermediate in the catalysis to form dialkyl ureas (Eq. (1)) [11]. Despite the formation of a mixture of products in the reaction of **1** with *p*-quinones, these oxidants may still be effective in catalytic reactions, because the product mixture reacts to form a species identified in catalytically active solutions and shown to produce urea upon thermolysis [34].

In a survey of reactions with other *p*-quinones, it was found that quinones substituted with electron-donating alkyl groups were less reactive than *p*-benzoquinone. For example, 2,5- and 2,6-dimethyl-*p*-benzoquinone were found to oxidize **1** very slowly as observed by IR spectroscopy. In addition, duroquinone was completely unreactive, possibly owing to the steric bulk about the carbonyl moieties. This is consistent with studies involving the reaction of **1** with substituted nitroaromatics which established the oxidation occurred by an inner sphere electron transfer mechanism [35].

Naphtho- and anthraquinone derivatives were also found to oxidize **1** slowly. The 1,4-naphthoquinone and 1,8-dichloroanthraquinone are more difficult to reduce than *p*-benzoquinone; their reduction potentials are similar to that of duroquinone. The reason they are reactive towards **1** while duroquinone is completely unreactive must be due to the reduced steric bulk at the carbonyl moieties in the annulated derivatives compared with the steric bulk caused by methyl substitution in duroquinone. Chloranil and 2,5-dichloro-*p*-benzoquinone were found to oxidize **1** completely within

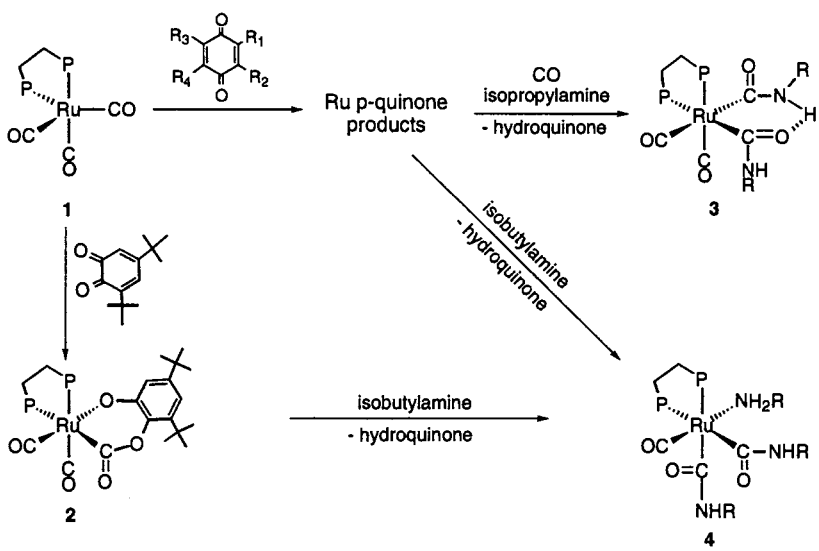

Scheme 1.

Table 3
Reactivity of substituted quinones with $Ru(dppe)(CO)_3$

Quinone	$E^a_{1/2}$	Reactivity with **1**[b]
p-Chloranil	0.01	Rapid
2,5-Dichloro-*p*-benzoquinone	−0.18	Rapid
p-Benzoquinone	−0.51	Moderate
3,5-Di-*t*-butyl-*o*-benzoquinone	−0.56	Moderate
2,5-Dimethyl-*p*-benzoquinone	−0.67	Slow
2,6-Dimethyl-*p*-benzoquinone	−0.67	Slow
1,4-Napthoquinone	−0.70	Slow
1,8-Dichloroanthraqui none	−0.76	Slow
Duroquinone	−0.84	No reaction
Anthraquinone	−0.94	No reaction

[a] Reduction potentials relative to SCE in MeCN.
[b] Time to reaction completion: rapid = min; moderate = 1–2 h, slow = not complete within 24 h.

minutes. This was evidenced by the appearance of peaks at higher ν_{CO} in the IR spectrum: 2054, 1992 cm^{-1} in the case of 2,5-dichloro*o*-*p*-benzoquinone and 2051, 1994 cm^{-1} in the reaction with *p*-chloranil. In addition, when isobutylamine was added to the oxidation reaction of *p*-chloranil and **1**, a single peak at 1915 cm^{-1} was observed in the IR spectrum and the ^{31}P spectrum exhibited a singlet at 40.0 ppm showing that a bis(carbamoyl) complex with a coordinated amine, $Ru(dppe)(CO)(RNH_2)[C(O)NHR]_2$ (**4**), was formed from the reaction (Scheme 1). The formation of **4** rather than **3** can be explained by the instability of **4** with amines which are disubstituted at the α-carbon. Therefore bulky amines, such as isopropylamine, lead to the formation of **3**, whereas amines which are monosubstituted at the α-carbon, such as isobutylamine, form **4**. The synthesis and characterization of the bis(carbamoyl) complexes have been discussed in separate publications [31,32]. The bis(carbamoyl) complex, **4**, is also believed to be an important catalytic intermediate in the formation of ureas [11].

A qualitative trend was noted by comparing the oxidation potential of Ru^0 with Ru^{+1}, which was previously determined to be +0.37V versus SCE in THF, [35] and the standard reduction potentials for the quinones (Table 3). The trend observed in the reactivity of **1** with these substituted quinones is that reactions which are exergonic, or slightly endergonic, went to completion within a couple of hours. If the reaction was unfavorable by more than ca. 0.2 V, then the reactions were quite slow and often did not go to completion. The mechanism of oxygen–atom transfer shown in Eq. 2

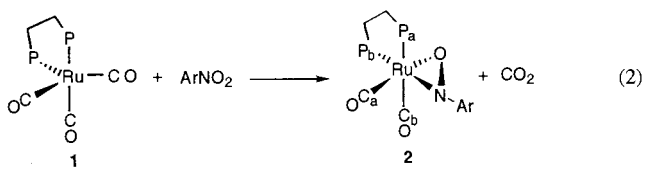

(2)

was found to involve an inner-sphere electron transfer and a quantitative correlation between $E_{1/2}$ of the nitroaromatics and the rate was established [35]. The possible intermediates of Eq. 2 are shown below.

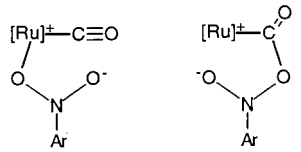

[Ru] = Ru(dppe)(CO)2

The qualitative trend outlined in Table 3 parallels that found for Eq. 2, and the structure of the *o*-quinone adduct is strikingly similar to the intermediates proposed for Eq. 2.

The reactivity of **1** was studied with 3,5-di-*t*-butyl-*o*-quinone in an attempt to isolate a stable ruthenium–quinone adduct. The reaction was rapid and proceeded cleanly; the elemental analysis of the product was consistent with 1:1 ruthenium–quinone adduct formation. The IR spectrum exhibited two carbonyl peaks of approximately equal intensity at 2051 and 1983 cm^{-1} corresponding to the terminal metal carbonyls, along with a weaker absorption at 1652 cm^{-1} corresponding to the acyl-type carbonyl of the metallacyclic ring. The ^{31}P-NMR spectrum of **2** showed doublets at 44.8 and 37.7 ppm with a coupling of 14 Hz between the two inequivalent phosphorus atoms. In the carbonyl region of the ^{13}C-NMR spectrum, the resonances at 201.5 ppm (dd, $J_{CP1} = 105.1$ Hz, $J_{CP2} = 10.3$ Hz) and 194.2 (dd, $J_{CP1} = 8.2$ Hz, $J_{CP2} = 97.6$ Hz) were consistent with two metal carbonyls, both of which are cis to one phosphine and trans to the other. A third resonance at 197.1 ppm (dd, $J_{CP} = 6.3$ Hz, $J_{CP} = 12.6$ Hz) was attributed to the carbonyl which was cis to both phosphines.

The structure of **2** is shown in Fig. 1, with relevant bond lengths and angles listed in Table 2. The geometry about ruthenium is distorted slightly from octahedral with a P1–Ru1–P2 bond angle of 82.45(6)° and a C3–Ru1–O5 bond angle of 85.7(2)°. The complex contains a non-planar, six-membered metallacyclic ring comprised of a carbonyl and a catecholate group. The ring is twisted with the catecholate moiety bent downward away from the bulky phosphine ligands. The ortho substituents of the aromatic ring are held in a nearly planar arrangement with a mean deviation of 0.02 Å from the plane of the phenyl ring.

The structure of **2**, was interesting in that the quinone had formally added across the ruthenium–carbon bond of a metal carbonyl resulting in a metallacyclic species with a carbonyl contained within the ring. Only one example of a similar reaction has been noted in the literature in which *o*-chloranil added to $[Rh(CO)L(\eta\text{-}C_5R_5)]$ (R = H, Me; L = CO, PPh_3) to form the product shown below [12].

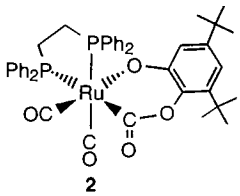

2

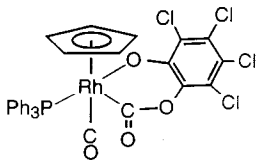

The formation of **2** from $Ru(dppe)(CO)_3$ was unexpected because the reactivity of trans-$Ru(PPh_3)_2(CO)_3$ with *o*-chloranil or tetrabromo-*o*-benzoquinone has been shown to involve the loss of one carbonyl ligand and the resulting product contains a catecholate ligand bound directly to ruthenium [16,20]. A similar product was observed when the radical cation, $Ru(PPh_3)_2(CO)_3^+$, was reacted with *o*-chloranil resulting in the loss of one CO and formation of the radical cation of the catecholate bound species shown above [36].

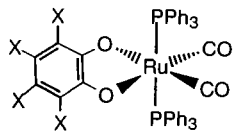

X = Cl, Br (Ref 16,20)

It was found that **2** reacts with isobutylamine to produce **4** cleanly (Scheme 1) as evidenced by a single peak in the ν_{CO} region of the IR spectrum at 1915 cm^{-1} and a singlet in the ^{31}P-NMR spectrum at 40.0 ppm. This is the same product which was observed from the reaction of isobutylamine with the unidentified *p*-quinone oxidation products. This similarity in reactivity of **2** suggests that the oxidation products from the reaction of **1** with *p*-quinones are also a 1:1 adduct between the ruthenium carbonyl and the *p*-quinone oxidant.

4. Supplementary material available

Tables of crystal structure data and structure refinement, positional parameters, thermal parameters, complete bond lengths and angles are available from author on request.

Acknowledgements

This research was funded by a grant from the National Science Foundation (CHE-9223433).

References

[1] F. L'Eplattenier, P. Matthys, F. Calderazzo, Inorg. Chem. 9 (1970) 342.
[2] Y. Tsuji, R. Takeuchi, Y. Watanabe, J. Organomet. Chem. 290 (1985) 249.
[3] J.J. Herman, A. Lecloux, Eur. Pat. Appl. EP 193982, 1986.
[4] T. Yoshida, N. Kambe, S. Murai, N. Sonoda, Bull. Chem. Soc. Jpn. 60 (1987) 1793.
[5] J.S. Lee, C.W. Lee, S.M. Lee, K. Park, J. Mol. Catal. 61 (1990) 15.
[6] S.M. Lee, N.S. Cho, K.D. Kim, J.S. Oh, C.W. Lee, J.S. Lee, J. Mol. Catal. 73 (1992) 43.
[7] C.W. Lee, J.S. Lee, S.M. Lee, K.D. Kim, N.S. Cho, J.S. Oh, J. Mol. Catal. 81 (1993) 17.
[8] T. Mizuni, Heteroatom Chem. 4 (1993) 455.
[9] M.M.T. Khan, S.B. Halligudi, S.H.R. Abdi, S. Shukla, J. Mol. Catal. 48 (1988) 25.
[10] P. Giannoccaro, J. Organomet. Chem. 470 (1994) 249.
[11] A.L. Jorgenson, W.L. Gladfelter (unpublished).
[12] N.G. Connelly, M.J. Freeman, I. Manners, A.G. Orpen, J. Chem. Soc. Dalton Trans. (1984) 2703.
[13] C.G. Pierpont, R.M. Buchanan, Coord. Chem. Rev. 38 (1981) 45.
[14] M. Pizzotti, S. Cenini, R. Ugo, F. Demartin, J. Chem. Soc. Dalton Trans. (1991) 65.
[15] A.L. Balch, J. Am. Chem. Soc. 95 (1973) 2723.
[16] A.Y. Girgis, Y.S. Sohn, A.L. Balch, Inorg. Chem. 14 (1975) 2327.
[17] B.K. Ghash, A. Chakravorty, Coord. Chem. Rev. 95 (1989) 239.
[18] M. Haga, E.S. Dodsworth, A.B.P. Lever, S.R. Boone, C.G. Pierpont, J. Am. Chem. Soc. 108 (1986) 7413.
[19] S.R. Boone, C.G. Pierpont, Inorg. Chem. 26 (1987) 1769.
[20] A.L. Balch, Y.S. Sohn, J. Organomet. Chem. 30 (1971) C31.
[21] D.S. Bohle, J. Chem. Soc., Chem. Commun. (1992) 1205.
[22] J.S. Field, R.J. Haines, J. Sundermeyer, M.W. Stewart, S.F. Woollam, J. Chem. Soc. Dalton Trans. (1992) 3161.
[23] S. Bhattacharya, Polyhedron 13 (1994) 451.
[24] N.G. Connelly, I. Manners, J.R.C. Protheroe, M.W. Whiteley, J. Chem. Soc. Dalton Trans. (1984) 2713.
[25] D.S. Bohle, K.T. Carron, A.N. Christensen, P.A. Goodson, A.K. Powell, Organometallics 13 (1994) 1355.
[26] N. Bag, G.K. Lahiri, P. Basu, A. Chakravorty, J. Chem. Soc. Dalton Trans. (1992) 113.
[27] J.E. Bäckvall, R.B. Hopkins, H. Grennberg, M.M. Mader, A.K. Awasthi, J. Am. Chem. Soc. 112 (1990) 5160.
[28] J.E. Bäckvall, A.K. Awasthi, Z.D. Renko, J. Am. Chem. Soc. 109 (1987) 4750.
[29] S.J. Skoog, A.L. Jorgenson, J.P. Campbell, M.L. Douskey, E. Munson, W.L. Gladfelter, J. Organomet. Chem. (in press).
[30] R.A. Sanchez-Delgado, J.S. Bradley, G. Wilkinson, J. Chem. Soc. Dalton Trans. (1976) 399.
[31] J.D. Gargulak, W.L. Gladfelter, Inorg. Chem. 33 (1994) 253.
[32] A.L. Jorgenson, B.K. Breedlove, J.D. Gargulak, J.P. Campbell, W.L. Gladfelter (unpublished).
[33] SHELXTL-Plus V5.0, v. 5.0; Madison, WI, 1995.
[34] J.D. Gargulak, W.L. Gladfelter, J. Am. Chem. Soc. 116 (1994) 3792.
[35] S.J. Skoog, W.L. Gladfelter, J. Am. Chem. Soc. 119 (1997) 11049.
[36] S.J. Sherlock, D.C. Boyd, B. Moasser, W.L. Gladfelter, Inorg. Chem. 30 (1991) 3626.